APL Materials

What controls electrostatic vs electrochemical response in electrolyte-gated materials? A perspective on critical materials factors

Cite as: APL Mater. **10**, 040901 (2022); https://doi.org/10.1063/5.0087396
Submitted: 04 February 2022 • Accepted: 14 March 2022 • Published Online: 04 April 2022

Chris Leighton, Turan Birol and Jeff Walter

What controls electrostatic vs electrochemical response in electrolyte-gated materials? A perspective on critical materials factors

Cite as: APL Mater. 10, 040901 (2022); doi: 10.1063/5.0087396
Submitted: 4 February 2022 • Accepted: 14 March 2022 •
Published Online: 4 April 2022

Chris Leighton,[1,a] Turan Birol,[1] and Jeff Walter[2]

AFFILIATIONS

[1] Department of Chemical Engineering and Materials Science, University of Minnesota, Minneapolis, Minnesota 55455, USA
[2] Department of Physics, Augsburg University, Minneapolis, Minnesota 55454, USA

[a] Author to whom correspondence should be addressed: leighton@umn.edu

ABSTRACT

Electrolyte-gate transistors are a powerful platform for control of material properties, spanning semiconducting behavior, insulator-metal transitions, superconductivity, magnetism, optical properties, etc. When applied to magnetic materials, for example, electrolyte-gate devices are promising for magnetoionics, wherein voltage-driven ionic motion enables low-power control of magnetic order and properties. The mechanisms of electrolyte gating with ionic liquids and gels vary from predominantly electrostatic to entirely electrochemical, however, sometimes even in single material families, for reasons that remain unclear. In this Perspective, we compare literature ionic liquid and ion gel gating data on two rather different material classes—perovskite oxides and pyrite-structure sulfides—seeking to understand which material factors dictate the electrostatic vs electrochemical gate response. From these comparisons, we argue that the ambient-temperature anion vacancy diffusion coefficient (*not* the vacancy formation energy) is a critical factor controlling electrostatic vs electrochemical mechanisms in electrolyte gating of these materials. We, in fact, suggest that the diffusivity of lowest-formation-energy defects may often dictate the electrostatic vs electrochemical response in electrolyte-gated inorganic materials, thereby advancing a concrete hypothesis for further exploration in a broader range of materials.

I. INTRODUCTION

Over the last decade or so, electrolyte gating has emerged as a powerful, versatile approach to electric-field- or voltage-based control of material properties.[1–3] The essential concept [one approach to which is illustrated in Fig. 1(a)] is to replace the oxide dielectric in a MOSFET (metal–oxide–semiconductor field-effect transistor) with an electrolyte, often an ionic liquid (IL). ILs are composed of bulky, asymmetric, typically organic cations and anions, with weak interactions, and thus, low melting point, rendering them liquid at room temperature with high ionic mobility.[1–3] When a positive gate voltage (V_g) is applied across such electrolytes [via a side gate in the example shown in Fig. 1(a)], mobile cations drift to the surface of the target, or channel material, which they typically cannot permeate [Fig. 1(b)]. The cations thus accumulate in a layer on the electrolyte side of the electrolyte/target material interface, generating an electric field. In the simplest picture [Fig. 1(b)], this field is then screened by the induction of an areal density of electrons on the target material side of the interface, forming an electric double-layer (EDL) and completing an electric double-layer transistor (EDLT).[1–3] The beauty of the EDLT is the large specific capacitance generated by the nanoscopic EDL (~10–100 μF cm^{-2}), which induces ~10^{14}–10^{15} cm^{-2} electron densities at just a few Volts, 10–100 times higher than in SiO_2-based MOSFETs.[1–3] The capacitance is also decoupled from the dielectric thickness, practically eliminating conventional leakage effects. Negative V_g inverts Fig. 1(b), bringing anions to the interface and inducing holes at the surface of the gated material.

The very large modulations in carrier density in EDLTs (often substantial fractions of an electron/hole per unit cell) make this a powerful approach for controlling not only electronic behavior, but also any carrier-density-dependent property, spanning magnetic, optical, and thermal.[1–26] While some usage pre-dates this, particularly in organic semiconductors,[1,4] the EDLT approach has thus

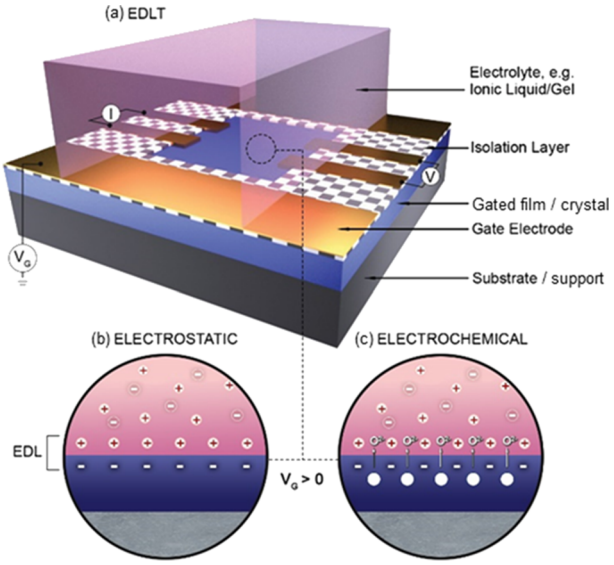

FIG. 1. (a) Schematic side-gate EDLT device. *I* and *V* are the current and voltage for channel resistance measurement; note that one of these electrodes is grounded. (b) and (c) Illustrations of (b) electrostatic and (c) electrochemical gating mechanisms. In (b), O^{2-} ions are being removed from the gated/target material (blue) to form V_O. Adapted with permission from C. Leighton, Nat. Mater. **18**, 13 (2019). Copyright 2018, Springer Nature Limited.

been broadly applied since ~2010, for control of semiconducting transport, insulator-metal transitions (IMTs), superconductivity, magnetism, and optical properties, across oxides, chalcogenides, 2D materials, organic conductors, and even elemental metals and alloys.[1–26] EDLTs have thus become an important tool in material research, typically applied to an initially insulating/semiconducting crystal,[5–7] or a thin film[8–24] or 2D material[25,26] on a substrate/support [Fig. 1(a)]. Improving the ease of fabrication and use of such devices, as well as their technological potential, *solid-state* ion gels (IGs) have been developed as electrolytes for EDLTs.[1,27] These IGs are essentially IL/polymer composites, offering high ionic mobility in easily processed solid-state materials.[1,27] In this Perspective, we focus specifically on such ionic-liquid- and ion-gel-based electrolytes, which, as noted above, have been used to good effect in many recent studies due to their high ionic mobility, wide electrochemical stability windows, and large EDL capacitance.[1–27]

II. ELECTROSTATIC AND ELECTROCHEMICAL GATING MECHANISMS

From over 10 years of quite intense activity with EDLTs, it is now unequivocal that electrolyte gating mechanisms are often far richer than the electrostatic induction of carriers depicted in Fig. 1(b).[3] Specifically, while some materials do respond predominantly electrostatically to ionic liquid or ion gel gating, various electrochemical mechanisms arise in other cases, which is unsurprising given the large interfacial electric fields generated.[3] In electrolyte gating of oxides, for example, a particularly well studied case, it is now established by multiple techniques (including *operando* scattering and spectroscopic probes, and experiments under O_2-rich/O_2-poor conditions) that application of positive V_g can remove O^{2-} ions from the gated oxide, creating oxygen vacancies (V_O) [Fig. 1(c)].[3,11–13,17,24,28–31] In the simplest model, the doubly positively charged V_O generate two free electrons, electron doping the oxide. The end result is thus similar to the electrostatic mechanism [Fig. 1(b)], but occurs via an entirely different (V_O-mediated) mechanism. A host of related gating mechanisms have now been detected in oxides and other materials, involving other V_g-induced vacancies [e.g., sulfur vacancies (V_S)[32]], insertion of H^+ ions generated by electrolysis of residual H_2O in ILs/IGs,[11,15,33] and even insertion of IL/IG ions themselves.[1,4,34] The latter can involve Li[35] or N ions,[36] for example, or, in polymer semiconductors, the V_g-driven insertion of organic ions.[1,4,34] Electrolyte gating mechanisms have thus been dubbed either "electrostatic," involving induction of electrons/holes [Fig. 1(b)] and ionic motion on only the electrolyte side of the interface, or "electrochemical," involving ionic motion on both sides of (and across) the interface [Fig. 1(c)].[3]

Significantly, electrochemical mechanisms realize some of the most striking, and potentially useful, electrolyte-gating-based modulations of properties.[10–13,15,17,28,29] Taking oxides as an example and focusing, in particular, on magnetoionics, perovskite cobaltite materials provide an ideal illustration. The goal of the nascent field of magnetoionics is low-power control of magnetic elements for data storage and processing applications, using voltage-driven ionic motion with little associated current for ultralow power applications.[3,37,38] Electrolyte gating is a good match to these goals and is thus widely applied in magnetoionic studies,[3,37,38] where perovskite cobaltites such as $SrCoO_3$ have recently emerged as particularly interesting.[10,11,15,39,40] This is because fully oxygenated perovskite $SrCoO_3$ is a ferromagnetic metal with a Curie temperature (T_C) around ambient (higher with Fe substitution[15]), while the oxygen-deficient V_O-ordered $SrCoO_{2.5}$ phase known as orthorhombic brownmillerite is an antiferromagnetic insulator with Néel temperature (T_N) ~ 570 K [see Fig. 2(a) for illustrations of the two crystal structures].[10,11,15] IL/IG gating of epitaxial films of $SrCoO_{3-\delta}$[11] (and related $La_{1-x}Sr_xCoO_{3-\delta}$[12,13,30] and $SrCo_{1-x}Fe_xO_{3-\delta}$[15]) proceeds via a strongly electrochemical mechanism, where reduction/oxidation at positive/negative V_g stabilizes the brownmillerite/perovskite phases, enabling V_g-based toggling between antiferromagnetic insulating and ferromagnetic metallic phases [Figs. 2(a)–2(c)]. Impressive modulations of magnetic, electronic, and optical properties are thus obtained, as shown in Figs. 2(b) and 2(c).[11,30] Figure 2(b), for example, contrasts the magnetization (M) vs field (H) behavior of $SrCoO_{3-\delta}$ films gated to perovskite and brownmillerite phases,[11] while Fig. 2(c) illustrates the fine V_g control of M vs temperature (T) that has been demonstrated in $La_{0.5}Sr_{0.5}CoO_{3-\delta}$.[30] Notably, the gate-induced redox in such cases is reversible, oxidation to perovskite from brownmillerite likely being facilitated by hydrolysis of residual H_2O in the ILs/IGs, providing the necessary source of oxygen.[3,11,15] This seems to be possible even in "dry" measurement environments such as moderate vacuum due to the retention of sufficient H_2O for this purpose in even nominally hydrophobic ILs.[11,41] Importantly, in such electrochemical mechanisms, the gating depth is not limited by the (typically nanoscopic) electrostatic screening length [as in Fig. 1(b)], but rather the diffusion length of O^{2-}/V_O, enabling gating of relatively thick (e.g., ~100 nm) films.[11,15,39] While important

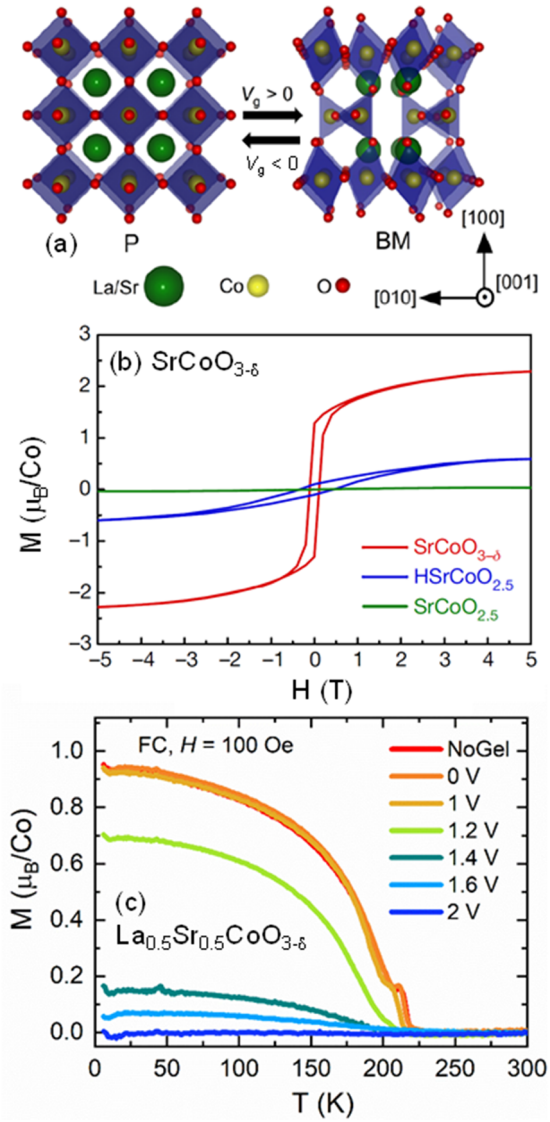

FIG. 2. (a) Perovskite ($La_{1-x}Sr_xCoO_3$) and brownmillerite ($La_{1-x}Sr_xCoO_{2.5}$) structures of (La,Sr)$CoO_{3-\delta}$. Note the ordered lines and planes of V_O in the brownmillerite. Adapted with permission from Chaturvedi *et al.*, ACS Appl. Mater. Interfaces **13**, 51205 (2021). Copyright 2021 American Chemical Society. (b) 10 K magnetization vs magnetic field for $SrCoO_{3-\delta}$ films gated to ferromagnetic perovskite (red) and antiferromagnetic brownmillerite (green) phases; also shown is $HSrCoO_{2.5}$ (blue), a third phase, achieved via H insertion. Adapted with permission from Lu *et al.*, Nature **546**, 124 (2017). Copyright 2017, Springer Nature. (c) Magnetization vs temperature for $La_{0.5}Sr_{0.5}CoO_{3-\delta}$ films gated (at the shown V_g) from the ferromagnetic perovskite to nonferromagnetic brownmillerite phases. Adapted with permission from Chaturvedi *et al.*, ACS Appl. Mater. Interfaces **13**, 51205 (2021). Copyright 2021 American Chemical Society.

issues remain to be fully resolved, including the ultimate limits on switching speed and endurance, such electrolyte-based electrochemical actuation thus appears to be promising for magnetionics and other fields, controlling magnetic, electronic, and optical function, for applications in neuromorphic and stochastic computing, tunable photonics, etc.[2,3,37,38] While in some cases (particularly organic devices[1]) soft solid electrolytes such as ion gels are ideal, in others, hard solid electrolytes may be preferable.[3] In this context, recent advances with gating using solid electrolytes and ionic conductors are particularly notable.[3,37,38,42,43]

While the above progress is impressive and has occurred rapidly, it also frames a question of substantial importance: *Why do some materials respond to ionic liquid or gel gating predominantly electrostatically [as in Fig. 1(b)], whereas others, sometimes even in the same family, respond electrochemically [as in Figs. 1(c) and 2(a)–2(c)]*? It is this issue that we tackle in this Perspective. This question is important not only for improved fundamental understanding of electrolyte gating mechanisms, but also because various critical application issues are impacted by these mechanisms, including switching speed, reversibility, and endurance.[1–3,37,38] One would thus like the ability to predict and tune electrolyte gating mechanisms in various materials. Seeking a high-level perspective of what material factors most strongly influence electrostatic vs electrochemical response to electrolyte gating, below, we compare gating of two quite different material classes: *perovskite oxides* and *pyrite transition-metal disulfides*. Through analysis of examples of predominantly electrostatic and electrochemical gating in these classes, we propose that one factor, anion vacancy diffusivity, significantly controls the extent of electrochemical response in these materials, and thus, the electrostatic/electrochemical gating balance. This generates a concrete hypothesis for further research, specifically that the ambient-temperature diffusivity of the lowest-formation-energy defects may be a broadly important factor in deciding electrostatic vs electrochemical response to electrolyte gating in inorganic materials.

III. EXAMPLE I: PEROVSKITE OXIDES

As already noted, oxides have proven to be a fertile ground for electrolyte gating and are some of the most intensively studied systems in this context. Oxide electrolyte gating mechanisms vary from predominantly electrostatic to almost entirely electrochemical, particularly, though not exclusively, through V_O formation/annihilation. Examples of oxides thought to gate predominantly electrostatically include ZnO,[8] In_2O_3,[44] In–Sn–O (ITO),[45] and $BaSnO_3$,[41,46] while strongly electrochemically responding oxides include TiO_2,[29] $SrTiO_3$,[28] $SrRuO_3$,[24] $La_{1-x}Sr_xMnO_3$,[47] and $SrCoO_{3-\delta}$ and related systems.[10–13,15,30,40] It should be noted here, as discussed further below, that this understanding is based in many cases on *operando* scattering and spectroscopy studies,[11,13,30,31,39,48] meaning that the conclusions of electrochemical response derive from direct probes. In Fig. 3, we focus our discussion by contrasting the published electrolyte gate response of two specific perovskites: wide-gap semiconducting $BaSnO_{3-\delta}$ (left) and magnetic $La_{1-x}Sr_xCoO_{3-\delta}$ (right). As will become clear, the response of epitaxial films of these materials to IL/IG-based gating is essentially diametrically opposite, meaning that they form a particularly instructive comparison.

Figures 3(a)–3(c) summarize the 300 K behavior (from Wang *et al.*[41]) of IG-gated epitaxial $BaSnO_{3-\delta}$ films with various thickness and initial *n*-type doping (achieved via La or V_O). The IG in this case is based on the IL [EMI][TFSI] [1-ethyl-3-methylimidazolium bis(trifluoro-methylsulfonyl) imide)] in a

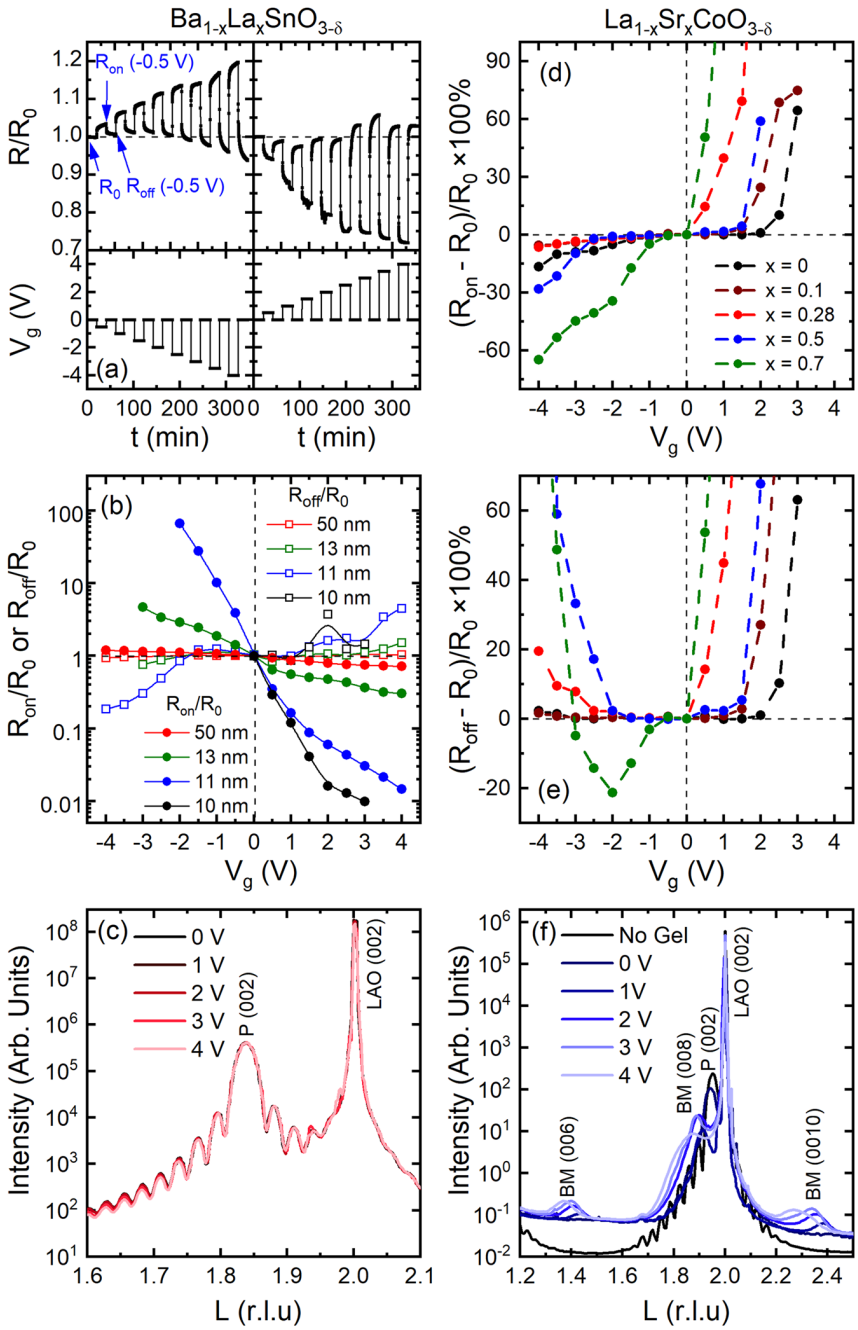

FIG. 3. Comparison of the V_g response of epitaxial films of $BaSnO_{3-\delta}$ (left) and $La_{1-x}Sr_xCoO_{3-\delta}$ (right) to IG gating. (a) Stepped gate voltage (V_g) vs time (t) for 50 nm-thick La-doped $BaSnO_{3-\delta}$ films (bottom), and the resulting 300 K resistance (R) response (top); the latter is normalized to the t = 0 resistance R_0. (b) V_g-dependent R_{on}/R_0 (solid points) and R_{off}/R_0 (open points), where R_{on} and R_{off} [illustrated in (a)] are at the end of the V_g application cycle and V_g removal cycle, respectively; 10, 11, and 12 nm films are V_O-doped, while 50 nm is La-doped. (c) 300 K *operando* (V_g-dependent) specular SXRD [vs substrate reciprocal lattice units (RLU)] for 14 nm-thick V_O-doped $BaSnO_3$. (d) and (e) V_g dependence of the 260 K gate-induced resistance change [$((R_{on} - R_0)/R_0) \times 100\%$] and non-volatility [$((R_{off} - R_0)/R_0) \times 100\%$] for 11 nm-thick $La_{1-x}Sr_xCoO_{3-\delta}$ films with various x. (f) 280 K *operando* (V_g-dependent) specular SXRD for 11 nm-thick x = 0.50 $La_{1-x}Sr_xCoO_{3-\delta}$ films. Perovskite (P) and brownmillerite (BM) peaks are labeled. Adapted with permission from Wang *et al.*, Phys. Rev. Mater. **3**, 075001 (2019). Copyright 2019 American Physical Society (left) and Chaturvedi *et al.*, ACS Appl. Mater. Interfaces **13**, 51205 (2021). Copyright 2021 American Chemical Society (right).

P(VDF-HFP) [poly(vinylidene fluoride-cohexafluoropropylene)] polymer network.[1,27] A common transport-based approach to elucidation of electrolyte gating mechanisms is shown in the bottom panel of Fig. 3(a), where progressively larger V_g magnitudes (both positive and negative) are cyclically applied and removed in a device similar to Fig. 1(a). Note that this is done slowly here (minute time scales) due to the side-gate geometry [Fig. 1(a)], which enables *operando* scattering studies (see below) but puts substantial distance between the gate and channel, greatly slowing device operation.[12,41] The top panel of Fig. 3(a) shows the resulting time (t) evolution of the resistance (R), normalized by the initial (t = 0) resistance (R_0). In $BaSnO_3$, this response to V_g is remarkably volatile and reversible, i.e., the resistance recovers to its initial value after bias removal. As shown in Fig. 3(a), positive V_g decreases R (as would be expected from additional electron doping in this n-type semiconductor) and negative V_g increases R (as would be expected for electron depletion), but R recovers to very close to its initial value after removal of each V_g, i.e., the gating is volatile, consistent with an electrostatic effect. This is reinforced in Fig. 3(b), which shows the V_g dependence of R_{on}/R_0 (solid points) and R_{off}/R_0 (open points), where R_{on} and R_{off} [see Fig. 3(a)] are the resistances with V_g applied and after V_g removal. These ratios quantify the gate effect and volatility, and are shown in Fig. 3(b) for films with varying thickness and initial doping. R_{on}/R_0 decreases with positive V_g (electron accumulation) and increases with negative V_g (electron depletion), with the overall gate effect increasing as the thickness is decreased. This is exactly as expected for electrostatic gating, where the depth scale is set by the Thomas–Fermi screening length (a few nm in this case).[3,14,41,46] At 11 nm thickness, R_{on}/R_0 varies between 10^2 and 10^{-2} between −2 and +4 V, i.e., a four-order-of-magnitude variation in 300-K R. Most importantly, the accompanying R_{off}/R_0 [open points in Fig. 3(b)] displays only minor excursions from 1, i.e., essentially volatile behavior. Some deviations from R_{off}/R_0 = 1 occur at low thickness but are much smaller than the effect of V_g on R_{on}/R_0 (solid points). Such transport studies thus support predominantly electrostatic electrolyte gating mechanisms in $BaSnO_3$,[41,46] as they do in the related $SrSnO_3$.[49]

Complementary *operando* synchrotron x-ray diffraction (SXRD) studies solidify the above conclusions.[41] As shown in Fig. 3(c), for example, application of V_g up to 4 V on the SXRD beamline (with *in situ* transport monitoring) induces no detectable structural modification (even with the extreme sensitivity of SXRD), a result that extends to negative V_g also.[41] This behavior stands in remarkable contrast to electrochemically responding oxides, as shown below. The evidence for predominantly electrostatic gating in $BaSnO_{3-\delta}$ is thus strong,[41] as it is in some other oxides.[8,44,45]

The drastically different behavior in perovskite $La_{1-x}Sr_xCoO_{3-\delta}$ is highlighted in Figs. 3(d)–3(f), which focus on IG-gated 11-nm-thick epitaxial films ($0 \le x \le 0.70$) from Chaturvedi *et al.*[30] The IG in this case is the same as for the $BaSnO_3$ experiments described above. Figures 3(d) and 3(e) first show the 260 K V_g dependence of $(\Delta R)_{gate} = [(R_{on} - R_0)/R_0 \times 100\%]$ and $(\Delta R)_{nv} = [(R_{off} - R_0)/R_0 \times 100\%]$, which quantify the gate effect and non-volatility, respectively, analogous to Figs. 3(a) and 3(b). The behavior at negative V_g is somewhat complex and we refer to Refs. 12–14 for a full discussion. More relevant here is the positive V_g behavior. Above an x-dependent threshold, $(\Delta R)_{gate}$ dramatically increases [Fig. 3(d)], but is accompanied by a quantitatively similar increase in $(\Delta R)_{nv}$ [Fig. 3(e)]. The gate effect is thus essentially entirely non-volatile [$(\Delta R)_{gate} \approx (\Delta R)_{nv}$], i.e., there is no recovery after returning V_g to 0. That this non-volatile positive-V_g gate effect occurs due to V_O formation was established relatively early on, via *operando* SXRD and polarized neutron reflectometry[13] (the latter confirming proliferation of V_O over 10s of nm depths), in addition to transport studies in O_2-rich/poor conditions.[12] Later work with *operando* x-ray absorption spectroscopy and x-ray magnetic circular dichroism provided further confirmation,[31] directly detecting the anticipated Co valence change. In essence, even at low V_g, the gate-induced V_O compensates the holes created by Sr doping, inducing large resistance increases. Consistent with the extensive work on $SrCoO_{3-\delta}$, *operando* SXRD by Chaturvedi *et al.*[30] [Fig. 3(f)] at higher V_g then detected a positive-bias-induced transformation from perovskite $La_{1-x}Sr_xCoO_{3-\delta}$ to brownmillerite $La_{1-x}Sr_xCoO_{2.5}$, enabling the electrical control of magnetism shown in Fig. 2(c). As already noted, in cobaltites, this transformation is strikingly reversible, with negative V_g application inducing reoxidation of antiferromagnetic brownmillerite to recover the ferromagnetic perovskite.[11,15,39] The evidence for strongly electrochemical (redox-based) electrolyte gating mechanisms in cobaltites is thus essentially unassailable.

Important insight into the electrochemical gating mechanisms in $La_{1-x}Sr_xCoO_{3-\delta}$ and related cobaltites was obtained by noting that these materials have low enthalpies of formation of V_O (ΔH_{Vo}) and extremely high V_O diffusion coefficients (D_{Vo}).[13,30] Electric-field-assisted V_O formation[50] could then be expected to be facile at the oxide/electrolyte interface [Fig. 1(c)], at which point, high D_{Vo} would enable depth-wise proliferation of V_O, eventually triggering the perovskite–brownmillerite transition.[30,51,52] Quantitatively, 300 K literature values for D_{Vo} in $La_{1-x}Sr_xCoO_{3-\delta}$ (~10^{-17} m^2 s^{-1}, Table I) imply diffusion lengths (l_{Vo}) of easily 100s of nm on the several minute time scales relevant to Figs. 3(d)–3(f) (Table I).[30,53–56] This is even without electric-field enhancement of V_O transport. Therefore, in simple terms, it is easy to both create and move V_O under V_g in electrolyte-gated $La_{1-x}Sr_xCoO_{3-\delta}$, enabling the results in Figs. 3(d)–3(f), and the similar ones in other cobaltites.[10–13,15,30,40] It is important to note here that, as in many perovskites, the enthalpy of formation of V_O in $La_{1-x}Sr_xCoO_{3-\delta}$ is generally substantially lower than other possible point defects, such as A- and B-site vacancies, interstitials, antisite defects, etc., explaining the particular importance of V_O in electrochemical gating.

Extending the above idea to $BaSnO_3$ is also revealing. Specifically, while ΔH_{Vo} in $BaSnO_{3-\delta}$ is again thought to be small/moderate

TABLE I. Measured/extrapolated 300 K anion vacancy diffusion coefficients (D_{Va}) and associated 30-min anion vacancy diffusion lengths (l_{Va}) for the four materials discussed in this study. Note that D_{Va} for $La_{1-x}Sr_xCoO_3$ is x-dependent; hence the range of values cited in that case. The D_{Va} data for $BaSnO_3$, $La_{1-x}Sr_xCoO_3$, FeS_2, and NiS_2 are from Refs. 59, 30, 66, and 65, respectively.

Material/class	D_{Va} (300 K) (m^2 s^{-1})	$l_{Va} = \sqrt{D_{Va}t}$, (t = 30 min) (m)
$BaSnO_3$/perovskite	10^{-31}	10^{-14}
$La_{1-x}Sr_xCoO_3$/perovskite	10^{-18}–10^{-16}	10^{-7}–10^{-6}
FeS_2/pyrite	10^{-37}	10^{-17}
NiS_2/pyrite	~10^{-10}	~10^{-4}

(thermal V_O doping is possible in both crystals and films[57,58]), D_{Vo} is *vastly* different to cobaltites, likely related to the large cation radii. Extrapolation of the reported D_{Vo} of $BaSnO_3$ to 300 K, in fact, yields extremely small values (~10^{-31} m^2 s^{-1}, Table I), corresponding to $l_{Vo} \ll 1$ Å on relevant time scales (Table I).[41,59] Electrolyte gating of $BaSnO_3$ thus occurs in a very different limit to $La_{1-x}Sr_xCoO_{3-\delta}$; while some electric-field-induced V_O formation *may* be possible in the top $BaSnO_3$ unit cell, for example (simple diffusion-equation-based analysis likely breaks down in this extreme l_{Vo} limit, however), proliferation of any induced V_O to significant depths appears implausible due to the highly limited V_O mobility. Given the very different behavior in Figs. 3(a)–3(c) vs Figs. 3(d)–3(f), this highlights an important correlation, which we now consider in a different class of materials.

IV. EXAMPLE II: PYRITE-STRUCTURE TRANSITION METAL SULFIDES

Recent data on electrolyte-gated pyrite-structure transition-metal disulfides[7,32] enable a test of the above ideas in a non-oxide, non-perovskite system. To this end, summarized in Figs. 4(a)–4(d) are transport data on IL-gated (with [EMI][TFSI]) single crystals (see insets for images) of FeS_2[7] and NiS_2,[32] respectively. For context, FeS_2 is a diamagnetic semiconductor (i.e., a band insulator) with a $t_{2g}^6 e_g^0$ electronic configuration, while NiS_2 is a $t_{2g}^6 e_g^2$ antiferromagnetic ($T_N \approx 38$ K) Mott insulator.[7,60,61] Figure 4(a) first shows the response of FeS_2 to increasing V_g, from 0 to 3 V (from Walter *et al.*[7]). The situation here is slightly complicated by the existence of a *p*-type surface conductive layer on FeS_2 crystals (in which the bulk is known to be natively *n*-doped by V_S[62]),[63,64] but the essential effect is clear: a dramatic decrease in low-T sheet resistance (R_s) occurs, signifying a V_g-induced surface insulator-metal transition (IMT). The latter is discussed in detail in Ref. 7, in which it was shown that this IMT is accompanied by surface ferromagnetism with induced T_C up to ~25 K. Notably, this is the first demonstration of voltage-induced ferromagnetism from a *diamagnetic* state, as opposed, for example, to voltage-induction of ferromagnetism from an antiferromagnetic state, as in cobaltites (discussed in Sec. III).[10,11,15] Most importantly in the current context, Fig. 4(b) shows that repeated cycling of IL-gated FeS_2 between 0 and 3 V establishes an essentially

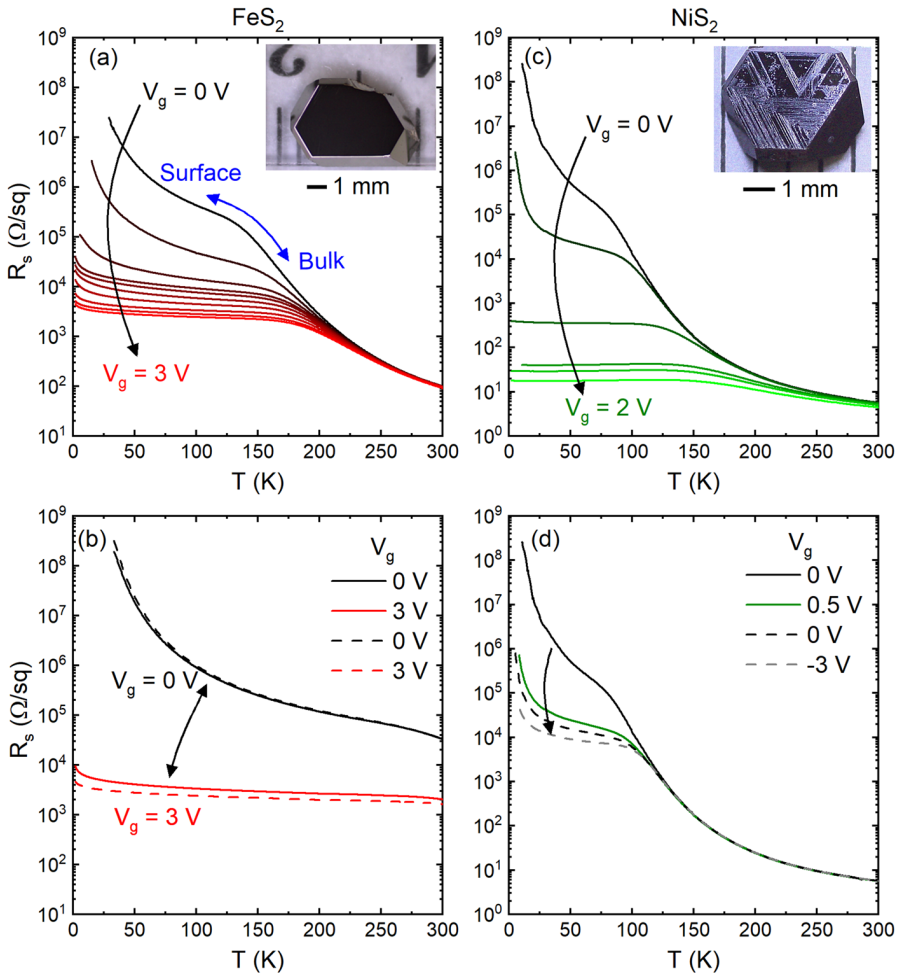

FIG. 4. Comparison of the response of single-crystal (see insets for images) FeS_2 (left) and NiS_2 (right) to IL gating. (a) Temperature (T) dependence of the sheet resistance (R_s) of FeS_2 for V_g of 0, 1.0, 1.1, 1.2, 1.3, 1.4, 1.6, 1.8, 2.0, and 3.0 V. As illustrated by the double-ended arrow, in the pristine state, the FeS_2 crystal interior frees out at low T, yielding to conduction via a more conductive surface layer. (b) FeS_2 $R_s(T)$ on cycling V_g between 0 and 3.0 V. (c) $R_s(T)$ of an NiS_2 crystal for V_g of 0, 0.5, 0.9, 1.3, 1.6, and 2.0 V. (d) NiS_2 $R_s(T)$ on cycling V_g from 0 to 0.5 V, back to 0, and then to −3 V. Adapted with permission from Walter *et al.*, Sci. Adv. **6**, eabb7721 (2020). Copyright 2020, American Association for the Advancement of Science (left) and Hameed *et al.*, arXiv:2201.00340 (2022).

entirely volatile and reversible gate effect. Returning V_g to zero, in fact, results in almost identical $R_s(T)$ to the initial state, despite the extreme sensitivity to the surface condition due to surface conduction. This is very strong evidence of a volatile, reversible, electrostatic gating mechanism. As an aside, we note that in this case, application of negative V_g from a pristine state induced very little resistance change, likely due to the high effective *p*-doping and low hole mobility in the surface layer. In essence, accumulation of additional holes on an already heavily *p*-doped surface has little impact, whereas inversion to *n*-type under positive bias does.

Figure 4(c) from the recent work of Hameed *et al.*[32] shows that IL-gated NiS_2 crystals exhibit what appears, at first sight, to be a similar V_g-induced IMT to FeS_2 [Fig. 4(a)]. Significantly, however, the low-T R_s in the NiS_2 case falls to as little as ~10 Ω at positive V_g, far beneath the quantum resistance [~26 kΩ, compare to Fig. 4(a)], strongly suggesting 3D, rather than 2D, conduction. Figure 4(d) shows that the gate response in this case is also strongly non-volatile and irreversible. Specifically, the large reduction in low-T R_s induced by 0.5 V is essentially entirely non-volatile when V_g is returned to 0, with even application of −3 V being unable to recover the initial insulating state. Consistent with this, depth-dependent energy-dispersive x-ray spectroscopy, x-ray photoelectron spectroscopy, and atomic force microscopy measurements by Hameed *et al.* revealed substantial reductions in the S:Ni ratio after gating, over 100s of nm depths.[32] The electrolyte gate effect in NiS_2 is thus strongly electrochemical, likely occurring initially via V_S formation in NiS_2, followed by reduction (in a depth-wise and laterally inhomogeneous fashion[32]) to lower S:Ni ratio compounds such as NiS, which are metallic, consistent with Fig. 4(c).[32] Figures 4(a) and 4(c) thus share resemblance, but the dominant gating mechanisms are, in fact, starkly different (near-ideally electrostatic in FeS_2 and strongly electrochemical in NiS_2). Note that unlike in our prior comparison of $BaSnO_3$ and $La_{1-x}Sr_xCoO_3$ (Sec. III), both FeS_2 and NiS_2 are transition-metal-based but, nevertheless, have very different electrolyte gating mechanisms.

In light of our conclusions from comparing $BaSnO_3$ and $La_{1-x}Sr_xCoO_3$, we now compare D_{Vs} values in FeS_2 and NiS_2. Before doing so, we note again that anion vacancies are known to be prevalent in these systems. As already noted, V_S are thought to be responsible for unintentional native doping of FeS_2 crystals,[62] and strong impacts of V_S on transport in NiS_2 have been claimed.[65] A comparison of the diffusivities of the V_S in these systems is revealing, however, as D_{Vs} in FeS_2 is notoriously low,[62,66] to the point of impeding certain approaches to V_S doping.[62] 300 K extrapolations are, in fact, so low (~10^{-37} m^2 s^{-1}, Table I) that they convert to truly negligible l_{Vs} on relevant time scales (≪1 Å, Table I), ruling out proliferation of any V_g-induced interfacial V_S, analogous to the situation with V_O in $BaSnO_3$. In NiS_2, on the other hand, potentially related to the expanded unit cell volume associated with its antiferromagnetic Mott insulating nature,[60,61,67] D_{Vs} is *vastly* larger (~10^{-10} m^2 s^{-1}, Table I).[65] The corresponding l_{Vs} are on *micrometer scales* (Table I), easily explaining the conspicuous gate-induced redox to 100s of nm depths in NiS_2.[32] We thus find in the pyrite disulfides another material system (this time entirely transition-metal-based) where the mobility of anion vacancies would appear to play an essential role in determining electrochemical vs electrostatic electrolyte gating mechanisms. Note here that in all such vacancy-mobility-based analyses, even if a highly conductive surface layer were to form, and thus screen the electric field, this would eliminate drift, but vacancy diffusion would remain active.

The *irreversibility* in Fig. 4(d), i.e., the inability to recover the initial state, also highlights an additional important finding from the disulfides. Specifically, unlike in the oxide case (due to residual H_2O), when electrochemical gating occurs in sulfides, there is no obvious sulfur source in the atmosphere (without chemical breakdown of a S-containing IL), disabling resulfidation to pyrite NiS_2 at negative V_g.[32] We emphasize here that it is known in oxide electrolyte gating that removed oxygen diffuses rapidly through the electrolyte and can thus escape the system (consistent with the sensitivity to O_2 atmospheric pressure[12,17,28,29]), and it is likely that this is true for sulfur also. The difference, however, is that in residual H_2O, the IL/IG has a reservoir for reoxidation of oxides, while no such reservoir exists for resulfidation of sulfides. This highlights an important point of distinction between oxides and sulfides, suggesting that reversible electrochemical gating of non-oxide chalcogenides, at least by sulfur removal/insertion with typical ILs/IGs, may be unlikely. Non-V_S-based reversible electrochemical gating mechanisms are possible in chalcogenides, for example, via Li^+ intercalation.[35]

V. OVERALL CONCLUSIONS, HYPOTHESES, AND FUTURE DIRECTIONS

The essential conclusion from the above analysis of literature data is that in the materials $BaSnO_3$, $La_{1-x}Sr_xCoO_{3-\delta}$, FeS_2, and NiS_2, which span perovskite oxides, pyrite disulfides, and both transition-metal- and non-transition-metal-based systems, the anion vacancy (V_a) diffusion coefficient (D_{Va}) is a critical parameter in dictating electrostatic vs electrochemical response to electrolyte gating. Quite surprisingly, the formation energy/enthalpy of these anion vacancies (ΔH_{Va}) does *not* seem to correlate with the electrostatic vs electrochemical electrolyte gate response. In $BaSnO_3$ and $La_{1-x}Sr_xCoO_{3-\delta}$, for example, the ΔH_{Vo} are thought to be not too different, and, notably, all of these materials ($BaSnO_3$, $La_{1-x}Sr_xCoO_{3-\delta}$, FeS_2, and NiS_2) can be readily V_a doped by thermal treatment or during growth.[13,57,58,62,65,68] This point was made as early as in the work of the Parkin group on materials such as VO_2[17] and TiO_2,[29] both of which respond to IL gating strongly electrochemically via V_O formation, despite the very high ΔH_{Vo} in rutile oxides.[69] Note that this is not to say that ΔH_{Va} has *no* impact on electrochemical gating. In $La_{1-x}Sr_xCoO_{3-\delta}$, for example, ΔH_{Vo} is strongly x-dependent, and this, indeed, impacts some *details* of the electrolyte gate response.[30] Specifically, ΔH_{Vo} decreases with x as the Co ions in $La_{1-x}Sr_xCoO_{3-\delta}$ evolve from 3+ to formally 4+, and this is known to significantly decrease the V_g threshold for the perovskite to brownmillerite transition.[30,51,52] Beyond $x \approx 0.7$, in fact, the threshold voltage becomes negligible and $La_{1-x}Sr_xCoO_{3-\delta}$ is typically in the brownmillerite phase as deposited and can be gated at negative V_g to the perovskite phase [as in Fig. 2(b)].[10,11,15] Below $x \approx 0.7$, on the other hand, $La_{1-x}Sr_xCoO_{3-\delta}$ can be straightforwardly deposited in the perovskite phase and gated at positive V_g to brownmillerite [as in Fig. 2(c)].[30] It is thus incorrect to say that ΔH_{Va} has *no* impact on electrochemical gating. Rather, more accurately, the question of electrostatic vs electrochemical response is simply far more significantly impacted by D_{Va} than ΔH_{Va}. Put another way, D_{Va} can apparently

be easily low enough to shut off electrochemical response to electrolyte gating by disabling proliferation of any induced interfacial V_a (as in $BaSnO_3$ and FeS_2), but even if ΔH_{Va} is very large (as in VO_2 and TiO_2), it is *not* sufficient to shut off electrochemical gate response. One could thus speculate that the interfacial electric field in EDLTs is essentially always able to lower ΔH_{Vo} to the point that V_O formation is facile, even in oxides with ΔH_{Vo} of many eV (as in TiO_2).

It should be emphasized, however, that, while we have drawn on the literature from a variety of oxides and sulfides, the above conclusions are based most heavily on the analysis of only four materials ($BaSnO_3$, $La_{1-x}Sr_xCoO_{3-\delta}$, FeS_2, and NiS_2) in only two classes (perovskite oxides and pyrite sulfides). Future work should, and no doubt will, go well beyond this, in various directions. In perhaps the most extensively studied case of oxides, for example, it is likely possible to devise means to *quantify* the extent of electrostatic vs electrochemical response to electrolyte gating, and then mine the literature for correlations with parameters such as D_{Vo}, ΔH_{Vo}, etc. Other potentially important factors such as the work function[70] and band alignment could be similarly considered. First principles computation could play an important role here, including through high-throughput calculations. Other low-formation-energy defects, such as H point defects, could also be treated in a similar fashion. More broadly, the hypotheses provided in this Perspective should also be more rigorously tested in non-oxide systems, including more sulfides, other chalcogenides, pnictides, and beyond. In such systems, it would be highly instructive to understand the hierarchy of formation energies of the possible point defects, to identify the lowest formation energy possibilities, and then to test the electrochemical response to electrolyte gating via formation and annihilation of these defects. If such results indeed correlate with the diffusivity of these lowest-formation-energy point defects, rather than their formation energies, this would support our hypothesis across a broader set of materials. Full establishment of such correlations would not only provide essentially the first rationalization of electrostatic vs electrochemical electrolyte gating tendencies in inorganic materials, but could even yield predictive capability for new materials. Considering the other side of the critical interface in electrolyte gating, it should also be emphasized that little has been done in terms of tailoring factors such as the IL ionic size and shape to control the interfacial electric field and its spatial modulation, which could potentially create entirely new means to control the balance between electrostatic and electrochemical responses in various materials. We hope that this Perspective will stimulate and guide future work in all of these directions.

VI. SUMMARY

In summary, we have contrasted literature data on ionic liquid and gel gating mechanisms in electrostatically and electrochemically responding perovskite oxides and pyrite-structure disulfides. These materials share commonalities but differ greatly in their oxygen/sulfur vacancy diffusion coefficients, leading to the hypothesis that this is a primary factor controlling the extent of electrochemical response in these materials, and thus, the electrostatic/electrochemical balance in their gating mechanisms. More generally, we hypothesize that the mobility of the lowest-formation-energy defects in inorganic materials (not the defect formation energies themselves) may well often dictate electrostatic vs electrochemical response to electrolyte gating. This provides a concrete hypothesis that, we hope, will now be more rigorously and quantitatively tested, in a wider variety of materials.

ACKNOWLEDGMENTS

This work was supported primarily by the National Science Foundation through the University of Minnesota MRSEC, under Grant No. DMR-2011401.

AUTHOR DECLARATIONS

Conflict of Interest

The authors have no conflicts to disclose.

Author Contributions

C.L., J.W., and T.B. developed the ideas presented in this Perspective. J.W. and C.L. prepared the figures and C.L. wrote the paper with input from J.W. and T.B.

DATA AVAILABILITY

The data in this Perspective were originally reported in Refs. 3, 7, 11, 30, 32, and 41 and should be obtainable from the relevant authors. The data that support the findings of this study are available from the corresponding author upon reasonable request.

REFERENCES

[1] S. H. Kim, K. Hong, W. Xie, K. H. Lee, S. Zhang, T. P. Lodge, and C. D. Frisbie, Adv. Mater. **25**, 1822 (2013).
[2] S. Z. Bisri, S. Shimizu, M. Nakano, and Y. Iwasa, Adv. Mater. **29**, 1607054 (2017).
[3] C. Leighton, Nat. Mater. **18**, 13 (2019).
[4] S. Chao and M. S. Wrighton, J. Am. Chem. Soc. **109**, 2197 (1987).
[5] K. Ueno, S. Nakamura, H. Shimotani, A. Ohtomo, N. Kimura, T. Nojima, H. Aoki, Y. Iwasa, and M. Kawasaki, Nat. Mater. **7**, 855 (2008).
[6] K. Ueno, S. Nakamura, H. Shimotani, H. T. Yuan, N. Kimura, T. Nojima, H. Aoki, Y. Iwasa, and M. Kawasaki, Nat. Nanotechnol. **6**, 408 (2011).
[7] J. Walter, B. Voigt, E. Day-Roberts, K. Heltemes, R. M. Fernandes, T. Birol, and C. Leighton, Sci. Adv. **6**, eabb7721 (2020).
[8] H. Shimotani, H. Asanuma, A. Tsukazaki, A. Ohtomo, M. Kawasaki, and Y. Iwasa, Appl. Phys. Lett. **91**, 082106 (2007).
[9] M. Nakano, K. Shibuya, D. Okuyama, T. Hatano, S. Ono, M. Kawasaki, Y. Iwasa, and Y. Tokura, Nature **487**, 459 (2012).
[10] Q. Lu and B. Yildiz, Nano Lett. **16**, 1186 (2016).
[11] N. Lu, P. Zhang, Q. Zhang, R. Qiao, Q. He, H.-B. Li, Y. Wang, J. Guo, D. Zhang, Z. Duan, Z. Li, M. Wang, S. Yang, M. Yan, E. Arenholz, S. Zhou, W. Yang, L. Gu, C.-W. Nan, J. Wu, Y. Tokura, and P. Yu, Nature **546**, 124 (2017).
[12] J. Walter, H. Wang, B. Luo, C. D. Frisbie, and C. Leighton, ACS Nano **10**, 7799 (2016).
[13] J. Walter, G. Yu, B. Yu, A. Grutter, B. Kirby, J. Borchers, Z. Zhang, H. Zhou, T. Birol, M. Greven, and C. Leighton, Phys. Rev. Mater. **1**, 071403(R) (2017).
[14] J. Walter, T. Charlton, H. Ambaye, M. R. Fitzsimmons, P. P. Orth, R. M. Fernandes, and C. Leighton, Phys. Rev. Mater. **2**, 111406(R) (2018).
[15] S. Ning, Q. Zhang, C. Occhialini, R. Comin, X. Zhong, and C. A. Ross, ACS Nano **14**, 8949 (2020).
[16] K. Shimamura, D. Chiba, S. Ono, S. Fukami, N. Ishiwata, M. Kawaguchi, K. Kobayashi, and T. Ono, Appl. Phys. Lett. **100**, 122402 (2012).
[17] J. Jeong, N. Aetukuri, T. Graf, T. D. Schladt, M. G. Samant, and S. S. P. Parkin, Science **339**, 1402 (2013).

[18]A. T. Bollinger, G. Dubuis, J. Yoon, D. Pavuna, J. Misewich, and I. Božović, Nature **472**, 458 (2011).
[19]X. Leng, J. Garcia-Barriocanal, S. Bose, Y. Lee, and A. M. Goldman, Phys. Rev. Lett. **107**, 027001 (2011).
[20]Y. Yamada, K. Ueno, T. Fukumura, H. T. Yuan, H. Shimotani, Y. Iwasa, L. Gu, S. Tsukimoto, Y. Ikuhara, and M. Kawasaki, Science **332**, 1065 (2011).
[21]A. S. Dhoot, C. Israel, X. Moya, N. D. Mathur, and R. H. Friend, Phys. Rev. Lett. **102**, 136402 (2009).
[22]L. M. Zheng, X. R. Wang, W. M. Lü, C. J. Li, T. R. Paudel, Z. Q. Liu, Z. Huang, S. W. Zeng, K. Han, Z. H. Chen, X. P. Qiu, M. S. Li, S. Yang, B. Yang, M. F. Chisholm, L. W. Martin, S. J. Pennycook, E. Y. Tsymbal, J. M. D. Coey, and W. W. Cao, Nat. Commun. **9**, 1897 (2018).
[23]D. Yi, Y. Wang, O. M. J. van't Erve, L. Xu, H. Yuan, M. J. Veit, P. P. Balakrishnan, Y. Choi, A. T. N'Diaye, P. Shafer, E. Arenholz, A. Grutter, H. Xu, P. Yu,B. T. Jonker, and Y. Suzuki, Nat. Commun. **11**, 902 (2020).
[24]H. T. Yi, B. Gao, W. Xie, S.-W. Cheong, and V. Podzorov, Sci. Rep. **4**, 6604 (2014).
[25]J. T. Ye, Y. J. Zhang, R. Akashi, M. S. Bahramy, R. Arita, and Y. Iwasa, Science **338**, 1193 (2012).
[26]I. Gutiérrez-Lezama, N. Ubrig, E. Ponomarev, and A. F. Morpurgo, Nat. Rev. Phys. **3**, 508 (2021).
[27]K. H. Lee, M. S. Kang, S. Zhang, Y. Gu, T. P. Lodge, and C. D. Frisbie, Adv. Mater. **24**, 4457 (2012).
[28]M. Li, W. Han, X. Jiang, J. Jeong, M. G. Samant, and S. S. P. Parkin, Nano Lett. **13**, 4675 (2013).
[29]T. D. Schladt, T. Graf, N. B. Aetukuri, M. Li, A. Fantini, X. Jiang, M. G. Samant, and S. S. P. Parkin, ACS Nano **7**, 8074 (2013).
[30]V. Chaturvedi, W. M. Postiglione, R. D. Chakraborty, B. Yu, W. Tabiś, S. Hameed, N. Biniskos, A. Jacobson, Z. Zhang, H. Zhou, M. Greven, V. E. Ferry, and C. Leighton, ACS Appl. Mater. Interfaces **13**, 51205 (2021).
[31]B. Yu, G. Yu, J. Walter, V. Chaturvedi, J. Gotchnik, S. Hameed, J. W. Freeland, C. Leighton, and M. Greven, Appl. Phys. Lett. **116**, 201905 (2020).
[32]S. Hameed, B. Voigt, J. Dewey, W. Moore, D. Pelc, B. Das, S. El-Khatib, J. Garcia-Barriocanal, B. Luo, N. Seaton, G. Yu, C. Leighton, and M. Greven, arXiv:2201.00340 (2022).
[33]H. Ji, J. Wei, and D. Natelson, Nano Lett. **12**, 2988 (2012).
[34]S. Wang, M. Ha, M. Manno, C. D. Frisbie, and C. Leighton, Nat. Commun. **3**, 1210 (2012).
[35]Y. Yu, F. Yang, X. F. Lu, Y. J. Yan, Y.-H. Cho, L. Ma, X. Niu, S. Kim, Y.-W. Son, D. Feng, S. Li, S.-W. Cheong, X. H. Chen, and Y. Zhang, Nat. Nanotechnol. **10**, 270 (2015).
[36]J. de Rojas, A. Quintana, A. Lopeandía, J. Salguero, B. Muñiz, F. Ibrahim, M. Chshiev, A. Nicolenco, M. O. Liedke, M. Butterling, A. Wagner, V. Sireus, L. Abad, C. J. Jensen, K. Liu, J. Nogués, J. L. Costa-Krämer, E. Menéndez, and J. Sort, Nat. Commun. **11**, 5871 (2020).
[37]C. Navarro-Senent, A. Quintana, E. Menéndez, E. Pellicer, and J. Sort, APL Mater. **7**, 030701 (2019).
[38]M. Nichterwitz, S. Honnali, M. Kutuzau, S. Guo, J. Zehner, K. Nielsch, and K. Leistner, APL Mater. **9**, 030903 (2021).
[39]B. Cui, P. Werner, T. Ma, X. Zhong, Z. Wang, J. M. Taylor, Y. Zhuang, and S. S. P. Parkin, Nat. Commun. **9**, 3055 (2018).
[40]D. A. Gilbert, A. J. Grutter, P. D. Murray, R. V. Chopdekar, A. M. Kane, A. L. Ionin, M. S. Lee, S. R. Spurgeon, B. J. Kirby, B. B. Maranville, A. T. N'Diaye, A. Mehta, E. Arenholz, K. Liu, Y. Takamura, and J. A. Borchers, Phys. Rev. Mater. **2**, 104402 (2018).
[41]H. Wang, J. Walter, K. Ganguly, B. Yu, G. Yu, Z. Zhang, H. Zhou, H. Fu, M. Greven, and C. Leighton, Phys. Rev. Mater. **3**, 075001 (2019).
[42]A. J. Tan, M. Huang, C. O. Avci, F. Büttner, M. Mann, W. Hu, C. Mazzoli, S. Wilkins, H. L. Tuller, and G. S. D. Beach, Nat. Mater. **18**, 35 (2019).
[43]C. Bi, Y. Liu, T. Newhouse-Illige, M. Xu, M. Rosales, J. W. Freeland, O. Mryasov, S. Zhang, S. G. E. te Velthuis, and W. G. Wang, Phys. Rev. Lett. **113**, 267202 (2014).
[44]W. Xie, X. Zhang, C. Leighton, and C. D. Frisbie, Adv. Electron. Mater. **3**, 1600369 (2017).
[45]X. Leng, A. T. Bollinger, and I. Božović, Sci. Rep. **6**, 31239 (2016).
[46]H. Wang, A. Prakash, K. Reich, K. Ganguly, B. Jalan, and C. Leighton, APL Mater. **8**, 071113 (2020).
[47]A. Molinari, P. M. Leufke, C. Reitz, S. Dasgupta, R. Witte, R. Kruk, and H. Hahn, Nat. Commun. **8**, 15339 (2017).
[48]A. M. Perez-Muñoz, P. Schio, R. Poloni, A. Fernandez-Martinez, A. Rivera-Calzada, J. C. Cezar, E. Salas-Colera, G. R. Castro, J. Kinney, C. Leon, J. Santamaria, J. Garcia-Barriocanal, and A. M. Goldman, Proc. Natl. Acad. Sci. U. S. A. **114**, 215 (2017).
[49]L. R. Thoutam, J. Yue, A. Prakash, T. Wang, K. E. Elangovan, and B. Jalan, ACS Appl. Mater. Interfaces **11**, 7666 (2019).
[50]M. Youssef, K. J. Van Vliet, and B. Yildiz, Phys. Rev. Lett. **119**, 126002 (2017).
[51]S. Zhang and G. Galli, npj Comput. Mater. **6**, 170 (2020).
[52]S. Zhang, H. Vo, and G. Galli, Chem. Mater. **33**, 3187 (2021).
[53]J. T. Mefford, X. Rong, A. M. Abakumov, W. G. Hardin, S. Dai, A. M. Kolpak, K. P. Johnston, and K. J. Stevenson, Nat. Commun. **7**, 11053 (2016).
[54]Y. Pan, X. Xu, Y. Zhong, L. Ge, Y. Chen, J.-P. M. Veder, D. Guan, R. O'Hayre, M. Li, G. Wang, H. Wang, W. Zhou, and Z. Shao, Nat. Commun. **11**, 2002 (2020).
[55]Y. Takeda, R. Kanno, T. Takada, O. Yamamoto, M. Takano, and Y. Bando, Z. Anorg. Allg. Chem. **540**, 259 (1986).
[56]F. R. van Buren, G. H. J. Broers, A. J. Bouman, and C. Boesveld, J. Electroanal. Chem. Interfacial Electrochem. **87**, 389 (1978).
[57]E. McCalla, D. Phelan, M. J. Krogstad, B. Dabrowski, and C. Leighton, Phys. Rev. Mater. **2**, 084601 (2018).
[58]K. Ganguly, A. Prakash, B. Jalan, and C. Leighton, APL Mater. **5**, 056102 (2017).
[59]W.-J. Lee, H. J. Kim, E. Sohn, H. M. Kim, T. H. Kim, K. Char, J. H. Kim, and K. H. Kim, Phys. Status Solidi **212**, 1487 (2015).
[60]S. Ogawa, S. Waki, and T. Teranishi, Int. J. Magn. **5**, 349 (1974).
[61]S. Ogawa, J. Appl. Phys. **50**, 2308 (1979).
[62]B. Voigt, W. Moore, M. Manno, J. Walter, J. D. Jeremiason, E. S. Aydil, and C. Leighton, ACS Appl. Mater. Interfaces **11**, 15552 (2019).
[63]M. Limpinsel, N. Farhi, N. Berry, J. Lindemuth, C. L. Perkins, Q. Lin, and M. Law, Energy Environ. Sci. **7**, 1974 (2014).
[64]J. Walter, X. Zhang, B. Voigt, R. Hool, M. Manno, F. Mork, E. S. Aydil, and C. Leighton, Phys. Rev. Mater. **1**, 065403 (2017).
[65]C. Clark and S. Friedemann, J. Magn. Magn. Mater. **400**, 56 (2016).
[66]E. B. Watson, D. J. Cherniak, and E. A. Frank, Geochim. Cosmochim. Acta **73**, 4792 (2009).
[67]S. El-Khatib, B. Voigt, B. Das, A. Stahl, W. Moore, M. Maiti, and C. Leighton, Phys. Rev. Mater. **5**, 115003 (2021).
[68]M. A. Torija, M. Sharma, J. Gazquez, M. Varela, C. He, J. Schmitt, J. A. Borchers, M. Laver, S. El-Khatib, and C. Leighton, Adv. Mater. **23**, 2711 (2011).
[69]A. Janotti, J. B. Varley, P. Rinke, N. Umezawa, G. Kresse, and C. G. Van de Walle, Phys. Rev. B **81**, 085212 (2010).
[70]A. B. Posadas, K. J. Kormondy, W. Guo, P. Ponath, J. Geler-Kremer, T. Hadamek, and A. A. Demkov, J. Appl. Phys. **121**, 105302 (2017).